IDENTIFICATION OF MOLECULES DERIVED FROM HUMAN FIBROBLAST FEEDER CELLS THAT SUPPORT THE PROLIFERATION OF HUMAN EMBRYONIC STEM CELLS

SERGEY V. ANISIMOV[1,2,3,*], NICOLAJ S. CHRISTOPHERSEN[1,*], ANA S. CORREIA[1,4], VANESSA J. HALL[1,5], INGRID SANDELIN[1,6], JIA-YI LI[1] and PATRIK BRUNDIN[1,§]

[1]Neuronal Survival Unit, Wallenberg Neuroscience Center, Department of Experimental Medical Science, Lund University, 221 84 Lund, Sweden,
[2]Research Department of Cell and Gene Engineering, V.A.Almazov Federal Center for Heart, Blood & Endocrinology, Saint-Petersburg, 197341, Russia,
[3]Department of Intracellular Signalling and Transport, Institute of Cytology, Russian Academy of Sciences, Saint-Petersburg, 194064, Russia,
[4]Faculty of Medicine, Centre de Recherche du CHUL, Neuroscience Axis, Université Laval, Québec, G1V4G2, QC, Canada,
[5]Department of Basic Animal and Veterinary Sciences, Faculty of Life Sciences, University of Copenhagen, Copenhagen, DK-1870, Denmark,
[6]IVF Kliniken Cura, 200 74 Malmö, Sweden.

*These authors contributed equally to this study.

Abstract: The majority of human embryonic stem cell lines depend on a feeder cell layer for continuous growth *in vitro*, so that they can remain in an undifferentiated state. Limited knowledge is available concerning the molecular mechanisms that underlie the capacity of feeder cells to support both the proliferation and pluripotency of these cells. Importantly, feeder cells generally lose their capacity to support human embryonic stem cell proliferation *in vitro* following long-term culture. In this study, we performed large-scale gene expression profiles of human foreskin fibroblasts during early, intermediate and late passages using a custom DNA microarray platform (NeuroStem 2.0 Chip). The microarray data was validated using RT-PCR and 'virtual SAGE' analysis. Our comparative gene expression study identified a limited number of molecular targets potentially involved in the ability of human neonatal foreskin fibroblasts to serve as 'feeder cells' for human embryonic stem cell culture. Among these, C-KIT, leptin and pigment epithelium-derived factor (PEDF) genes were the most interesting candidates.

Key Words: Human embryonic stem cells, Feeder cells, DNA Microarray.

[§]**Author for correspondence**: Patrik Brundin, Neuronal Survival Unit, Wallenberg Neuroscience Center, Department of Experimental Medical Science, Lund University, BMC A10, Sölvegatan 17, 221 84 Lund, Sweden. Phone: +46-46-2220525; Fax: +46-46-2220531; e-mail: patrik.brundin@med.lu.se

Abbreviations used: hESC – human embryonic stem cells; hFC – human fibroblast cells; hFF – human neonatal foreskin fibroblasts; HPC – hematopoietic progenitor cells; HSC – hematopoietic stem cells; MEF – mouse embryonic fibroblasts; MSC – mesenchymal stem cells; NSC – neural stem cells; SAGE – serial analysis of gene expression.

INTRODUCTION

Embryonic stem cells (ESC) were first derived from the inner cell mass of the murine blastocyst in 1981 [1]. Such cell lines were also later produced using human embryos [2]. Today, human ESC (hESC) are used for basic research to provide invaluable insight into the mechanisms underlying cell proliferation, differentiation, aging and regeneration. Current scientific efforts

aim to move hESC-based technology from experimental research into the clinic. Most hESC lines are maintained on a feeder layer of separate origin. Mouse embryonic fibroblast (MEF) feeder cells were traditionally used to support the derivation and expansion of hESC lines. However, due to the risks, which include transmission zoonosis, a more clinical approach is required, so that the hESC are not exposed to xenogenic factors. Thus, feeder-free approaches have been developed. These include the supplementation of a high concentration of exogenous fibroblast growth factor 2 (FGF2); the addition of transforming growth factor β (TGFβ) and noggin proteins; the use of a matrix (such as Matrigel); or a combination of these approaches. Using defined media (e.g. mTeSR1 and mTeSR2 [3]) is also now widespread and allows for the effective expansion of hESC in feeder-free conditions. Despite these advances, the culturing of hESC on feeder cells of human origin, i.e. human fibroblast cells (hFC) [4], is still used for *in vitro* culturing and the expansion of some hESC lines (though feeder layers of mouse origin are used even more extensively). hFC have a number of advantages over mouse embryonic fibroblasts (MEF), both with regards to safety and convenience. Numerous hFC cell types have been used, but human neonatal foreskin fibroblasts (hFF) appear to be the most commonly used human feeder cell type worldwide.

The mechanisms underlying hESC-supporting feeder cell properties are currently not known in detail, but are suggested to be related to i) the secretion of factors into the culture media and/or ii) the expression of certain molecules over the cell surface membrane of hFC. Interestingly, fibroblasts (including MEF and hFF) can only support hESC proliferation *in vitro* during their early cell passages; spontaneous differentiation and cell death become evident in hESC plated on late passage hFC [5, 6]. Therefore, we hypothesized that comparing large-scale gene expression profiles of hFF during early, intermediate and late passages (i.e. the passages able and unable to support hESC proliferation *in vitro*) using a custom microarray platform [7] could identify factors underlying the ability of hFF to support the self-renewal of hESC. Once identified, those factors could provide essential insight into the general biology of ESC and contribute to the establishment of more well-defined 'feeder-free' protocols for culture of hESC.

MATERIALS AND METHODS

Human neonatal foreskin fibroblast cells (hFF) were obtained from a commercial source (ATCC; cell line CCD-1112Sk) and expanded in hFF medium (IMDM, Invitrogen, USA) supplemented with 10% heat-inactivated FCS (Invitrogen) and 0.5% Penicillin/Streptomycin (Invitrogen) in regular culture conditions. Human embryonic stem cells (hESC; SA002 line, Cellartis AB, Göteborg, Sweden) were co-cultured with mitotically inactivated (40 Gy) hFF in the presence of 4 ng/ml human recombinant FGF2 (Biosource International, USA) to assess the latter cells' ability to support hESC proliferation *in vitro* in an undifferentiated stage. Cells were harvested for RNA isolation from hFF at sub-confluency during passages 6-15, 20, 25, 30 and 34, then purified following the RNeasy Kit protocol (QIAGEN, USA), with DNase I treatment (QIAGEN). RNA integrity was tested using both an ND-1000 spectrophotometer (NanoDrop, USA) and RNA Nano LabChip/2100 Bioanalyzer system (Agilent Technologies, USA). Total RNA for Sample I and Sample II was prepared by pooling equal quantities of individual total RNA samples from cells during passages 6-11 and 12-15, respectively. The fluorescent label incorporation was performed using a Low RNA Input Fluorescent Linear Amplification Kit (Agilent Technologies, USA); Human Universal Reference RNA (Stratagene, USA) and dye-swap replicate amplification were used. The properties of the 'NeuroStem' custom microarray platform are described extensively in [7]. Briefly, the NeuroStem 2.0 Chip platform accounts for a total of 11532 individual oligonucleotides (69-71 nucleotides long), including 1312 oligonucleotides that match genes related to the growth and differentiation of stem cells, further supplemented with a large number of controls (in particular, for data normalization). All of the unique genes were spotted in quadruplicate over the same slide. Arrays were produced by the SweGene DNA Microarray Resource Centre, Department of Oncology at Lund University

(Sweden) using a MicroGrid II 600R arrayer (Harvard BioRobotics, USA). For a detailed protocol of the platform manufacturing, application and analyses, see the Supplementary Materials and Methods. Microarray data validation included RT-PCR, SAGE cross-library analysis and ELISA (see the Supplementary Materials and Methods).

RESULTS

In concordance with the results of previous research [4, 5], we observed that a high rate of proliferation and a low grade of spontaneous differentiation in hESC cultures could not be achieved with hFF older than passages 11-12. The hFF derived from later passages were unable to support hESC proliferation *in vitro*, and the rate of spontaneous differentiation increased gradually, finally approaching 100%, co-inciding with massive cell death (Suppl. Figs 1 and 2). Using laboratory records, we retrospectively analyzed the growth rates of hFF routinely used to support hESC in our laboratory (raw data from >200 passages). We observed that the hFF appear morphologically unaltered (i.e. do not appear hypertrophic) and display an equal growth rate from passage 4 to 25. Morphological changes become evident in hFF only by passage 25 (Suppl. Figs 3 & 4). We therefore hypothesized that it is between passages 12 and 25 that hFF may undergo molecular changes which lead to the loss of their ability to support hESC proliferation.

To identify the molecular expression changes in aging fibroblasts, hFF were cultured for up to 35 passages, and RNA samples were purified and tested for integrity. The following hFF samples were selected for the microarray study using a custom oligonucleotide microarray platform (NeuroStem 2.0 Chip):

(I) Passages 6-11 (i.e. hFF able to support hESC proliferation);

(II) Passages 12-20 (i.e. unable to support hESC proliferation, but morphologically unaltered and with same growth rate as in Passages 6-11);

(III) Passage 25 (i.e. morphologically altered but with the same growth rate as in Passages 6-20); and

(IV) Passage 30 (i.e. severely morphologically altered, with a lower growth rate than Passage 6-25).

Using a conservative set of criteria, we were able to identify a group of 232 gene targets (2.01% of the total number of genes screened) with an expression in Sample I that is significantly different to that in Samples II-IV. In the latter Samples, a significant group of genes were related to the cell cycle, most likely responsible for the replicative aging process occurring in the hFF, although not reflected in the growth rate at this stage. Six genes encoding secreted molecules and one gene controlling secretion were identified among the gene targets (Tab. 1), including pigment epithelium-derived factor (*PEDF*; serpin peptidase inhibitor, clade F member 1; α2 antiplasmin; also used to be known as *EPC1*) and leptin (*LEP*; Fig. 1). Moreover, there were 43 additional gene products with expressions different in Sample I vs. Samples II-IV that were related to cell surface membrane (Suppl. Tab. 1, Fig. 2), including *C-KIT* (also known as *CD117* and mast/stem cell growth factor receptor (*SCFR*)).

In a subsequent analysis, we matched the target list to the GEO (Gene Expression Omnibus) database (NCBI), in which 3 entries related to 'feeder cells' are available to the scientific community. The Serial Analysis of Gene Expression (SAGE) libraries of primary (passage 0) human foreskin cells (GSM1), those of passages 15-18 (GSM14916); and the MEFs of passage 3 (GSM7759; [8]) were downloaded, and SAGE tags for the corresponding gene targets were identified using SAGE Map software (NIH). Targets identified using the NeuroStem Chip were matched to those libraries. Importantly, a large proportion of gene targets identified using microarray technology (including secreted, secretion-related and cell surface membrane-related ones) were also identified in the SAGE libraries: 142 redundant tags for *Homo sapiens*, matching 42 unique genes; and 137 redundant tags for *Mus musculus*, matching 45 unique genes were identified for 50 target genes tested. Of those tags, 42 (matching 33 unique genes) were expressed in the human GSM1 and GSM14916 SAGE libraries, and 29 (matching 24 unique

genes) were expressed in the mouse GSM7759 SAGE library. Suppl. Tab. 2 lists 37 unique genes encoding secreted, secretion-related and cell surface membrane-related products identified in one of the three SAGE libraries analyzed.

The normalized abundance of the individual tags was also compared between human feeder cell-derived SAGE libraries approximately corresponding to Sample I and Sample II of our experiment. The resulting trends were compared to that derived from microarray analysis (Suppl. Fig. 5). Despite the principally different manners in which the data was generated, in a number of cases, we were able to observe high levels of similarity between the expression patterns observed in our microarray experiments (Tab. 1, Suppl. Tab. 1) and in human SAGE feeder cell-derived libraries.

To further validate the gene expression changes observed in the microarray experiments, we performed RT-PCR analysis. Herein, the expression of a number of selected target genes was investigated in a wide range of hFF-derived samples (passages 6-15, 20, 25, 30, 34; thus exceeding the assay of raw samples assessed in the microarray experiments). In particular, in concordance with microarray data, RT-PCR demonstrated that the expression of *C-KIT* and *LEP* rapidly dropped with hFF passage number. A wider range of hFF samples allowed us to identify with higher precision that the expression of *C-KIT* and *LEP* decreased after passage 9 and nearly completely disappeared after passage 25 (Suppl. Fig. 6). Furthermore, using ELISA, we confirmed that the levels of secreted PEDF declined over increasing passage number. The linear regression curve obtained for the PEDF antigen had an R2 value of 0.943. The normalized PEDF values were 16 ng/ml, 12.16 ng/ml and 11.52 ng/ml for passage numbers 9, 16, and 21, respectively.

DISCUSSION

It is generally recognized that feeder cells (including MEF and hFF) are only able to support the proliferation of hESC in an undifferentiated condition for a limited number of passages, from 11-12 to 15 for hFF [3, 4] and from 3-4 to 6-7 for MEF [9]. However, little is known about the basic mechanisms underlying the hESC-supportive features of either type of feeder cell. In this study, we aimed to identify genes that may encode molecules supportive for the proliferation and pluripotency of hESC. Using a custom microarray platform, we identified a limited number of 232 gene targets with expressions that were significantly between hFF passages termed early (passage numbers $\leq$ 11) and late (passage numbers > 11). We obtained support for our microarray-generated data using RT-PCR studies and 'virtual SAGE', based upon the analysis of expression of selected genes in an array of publicly available SAGE libraries. Notably, a degree of overlap between the available human libraries and across species (including that for secretion- and cell surface membrane-related genes) supports the notion that the mechanisms underlying the ability of human and murine feeder cells to support hESC proliferation might be identical.

As expected, a significant group of gene targets identified in our study was related to the cell cycle, in concordance with the aging process in hFF. Similarly, a limited group of identified gene targets (50 genes) was related either to cell secretion (i.e. encoding secreted molecules or controlling secretion), or to the cell surface membrane (Tab. 1 and Suppl. Tab. 1). Several studies suggest that the hESC-supportive features of fibroblasts are primarily (or even entirely) based on secreted factors [10, 11]. Therefore, we investigated the group of genes encoding the secreted proteins. Among the latter, we identified vitronectin (*VTN*), serine protease 23 (*PRSS23*), Wingless-type MMTV integration site family member 2 (*WNT2*), tumor necrosis factor receptor superfamily member 1A (*TNFRSF1A*), pigment epithelium-derived factor (*PEDF)* and leptin (*LEP*). Additionally, the homeobox D4 (*HOXD4*) gene, believed to affect the secretion process, was also identified. Importantly, only two of those genes, *PEDF* and *LEP*, were consistently down-regulated throughout replicative senescence (Fig. 1).

It is now recognized that leptin inhibits apoptosis and enhances cell proliferation via specific activation of certain signalling pathways. Leptin and the leptin receptor are expressed in

fibroblasts, and it has been observed that leptin receptors are expressed in various stem cell types, including human mesenchymal stem cells (hMSC), haematopoietic stem and progenitor cells (hHSC, hHPC) and hESC [7]. Similarly, PEDF function has been linked to the maintenance of stem cell populations, namely that of neural stem cells (NSCs) [12]. PEDF is also considered to be involved in the maintenance of adult 'niches' of NSCs and to promote their proliferation via the activation of signalling pathways, while a blockade of endogenous PEDF decreases the proliferation [12]. Most interestingly, a few independent studies have linked alterations of PEDF expression in human fibroblast and fibroblast-like cells undergoing replicative senescence [13-15], which illustrates that senescent cells may not be able to produce PEDF transcripts. Previous studies have identified PEDF in mouse and human fibroblast cell-conditioned medium, suggesting that this protein could also be a potential regulator of hESC. Finally, in a more recent study, it was firmly established that PEDF supports the self-renewal of pluripotent hESC, promoting long-term growth of pluripotent hESC *in vitro* without further bFGF or TGFβ/Activin/Nodal ligand supplementation [16].

To fulfill their role in supporting stem cells, the secreted factors PEDF and leptin could utilize partial synergistic mechanisms, since both are recognized activators of the mitogen-activated protein kinase (MAPK) signalling cascade. This cascade potentially involves yet another factor identified in our study, namely C-KIT. This factor represents the sole entry in the group of cell surface membrane-related molecules which is linked not only to germ cell precursors and stem cell subtypes, but also to the MAPK signalling pathway and to leptin itself [17, 18]. We hypothesize that the PEDF, leptin and C-KIT-mediated systems may play important roles in controlling the 'hESC-supportive' features of hFF, while other molecular mechanisms may also be involved. Among these is the well-documented FGF2 pathway, while others remain to be identified. We strongly believe that performing a similar analysis with various types of fibroblast cells (including MEF and human fibroblasts of various biological origin) and follow-up functional analyses of the identified molecular targets (as applied to the assay of hESC cell lines), could help to identify these. Using available feeder-free cell expansion systems (including mTeSR1 and mTeSR2 media) could be most useful in this context. This would be indeed most useful for the further development of feeder-free/xeno-free methods of hESC expansion.

ACKNOWLEDGEMENTS

Please write the names in full in the acknowledgements. Do not use initials.

Sergey V. Anisimov's work is supported by the MCB Program, Russian Academy of Sciences and NordForsk (Grant No. 080250). Nicolaj S. Christophersen is sponsored by a grant from Lundbeckfonden (#R7-A686). Ana S. Correia is supported by Fundação para a Ciência e Tecnologia (ref SFRH/BD/11804/2003).

REFERENCES

1. Evans, M.J. and Kaufman, M.H. Establishment in culture of pluripotential cells from mouse embryos. **Nature.** 292 (1981) 154–156.
2. Thomson, J.A., Itskovitz-Eldor, J., Shapiro, S.S., Waknitz, M.A., Swiergiel, J.J., Marshall, V.S. and Jones, J.M. Embryonic stem cell lines derived from human blastocysts. **Science.** 282 (1998) 1145-1147.
3. Ludwig T.E., Levenstein M.E., Jones J.M., Berggren W.T., Mitchen E.R., Frane J.L., Crandall L.J., Daigh C.A., Conard K.R., Piekarczyk M.S., Llanas R.A. and Thomson J.A. Derivation of human embryonic stem cells in defined conditions. **Nature Biotechnology.** 24 (2006) 185-187.

4. Richards, M., Fong, C.Y., Chan, W.K., Wong, P.C. and Bongso, A. Human feeders support prolonged undifferentiated growth of human inner cell masses and embryonic stem cells. **Nat. Biotechnol.** 20 (2002) 933-936.
5. Unger, C., Felldin, U., Nordenskjöld, A., Dilber, M.S. and Hovatta, O. Derivation of human skin fibroblast lines for feeder cells of human embryonic stem cells. **Curr. Protoc. Stem Cell Biol.** (2008) Chapter 1:Unit 1C.7.
6. Panula, S. and Reijo Pera, R.A. Preparation of human foreskin fibroblasts for human embryonic stem cell culture. **Cold Spring Harb. Protoc.** (2008) doi:10.1101/pdb.prot5043.
7. Anisimov, S.V., Christophersen, N.S., Correia, A.S., Li J.Y. and Brundin, P. "NeuroStem Chip": a novel highly specialized tool to study neural differentiation pathways in human stem cells. **BMC Genomics.** 8 (2007) 46.
8. Wiese, C., Rolletschek, A., Kania, G., Navarrete-Santos, A., Anisimov, S.V., Steinfarz, B., Tarasov, K.V., Brugh, S.A., Zahanich, I., Rüschenschmidt, C., Beck, H., Blyszczuk, P., Czyz, J., Heubach, J.F., Ravens, U., Horstmann, O., St-Onge, L., Braun, T., Brüstle, O., Boheler K.R. and Wobus, A.M. Signals from embryonic fibroblasts induce adult intestinal epithelial cells to form nestin-positive cells with proliferation and multilineage differentiation capacity in vitro. **Stem Cells.** 24 (2006) 2085-2097.
9. McElroy, S.L. and Reijo Pera, R.A. Preparation of mouse embryonic fibroblast feeder cells for human embryonic stem cell culture. **Cold Spring Harb. Protoc.** (2008) doi:10.1101/pdb.prot5041.
10. Chin, A.C., Fong, W.J., Goh, L.T., Philp, R., Oh, S.K. and Choo, A.B. Identification of proteins from feeder conditioned medium that support human embryonic stem cells. **J. Biotechnol.** 130 (2007) 320-328.
11. Montes, R., Ligero, G., Sanchez, L., Catalina, P., de la Cueva, T., Nieto, A., Melen, G.J., Rubio, R., García-Castro, J., Bueno, C., Menendez, P. Feeder-free maintenance of hESCs in mesenchymal stem cell-conditioned media: distinct requirements for TGF-beta and IGF-II. **Cell Res.** 19 (2009) 698-709.
12. Ramirez-Castillejo, C., Sanchez-Sanchez, F., Andreu-Agullo, C., Ferron, S.R., Aroca-Aguilar, J.D., Sanchez, P., Mira, H., Escribano, J. and Farinas, I. Pigment epithelium-derived factor is a niche signal for neural stem cell renewal. **Nat. Neurosci.** 9 (2006) 331-339.
13. Coljee, V.W., Rotenberg, M.O., Tresini, M., Francis, M.K., Cristofalo, V.J. and Sell, C. Regulation of EPC-1/PEDF in normal human fibroblasts is posttranscriptional. **J. Cell. Biochem.** 79 (2000) 442-452.
14. Kojima, T., Nakahama, K., Yamamoto, K., Uematsu, H. and Morita, I. Age- and cell cycle-dependent changes in EPC-1/PEDF promoter activity in human diploid fibroblast-like (HDF) cells. **Mol. Cell. Biochem.** 293 (2006). 63-69.
15. Pignolo, R.J., Rotenberg, M.O. and Cristofalo, V.J. Analysis of EPC-1 growth state-dependent expression, specificity, and conservation of related sequences. **J. Cell. Physiol.** 162 (1995) 110-118.
16. Gonzalez, R., Jennings, L.L., Knuth, M., Orth, A.P., Klock, H.E., Ou, W., Feuerhelm, J., Hull, M.V., Koesema, E., Wang, Y., Zhang, J., Wu, C., Cho, C.Y., Su, A.I., Batalov, S., Chen, H., Johnson, K., Laffitte, B., Nguyen, D.G., Snyder, E.Y., Schultz, P.G., Harris, J.L., Lesley, S.A. Screening the mammalian extracellular proteome for regulators of embryonic human stem cell pluripotency. **Proc. Natl. Acad. Sci. USA.** 107 (2010) 3552-3557.
17. Attoub, S., Rivat, C., Rodrigues, S., Van Bocxlaer, S., Bedin, M., Bruyneel, E., Louvet, C., Kornprobst, M., Andre, T., Mareel, M., Mester, J. and Gespach, C. The c-kit tyrosine kinase inhibitor STI571 for colorectal cancer therapy. **Cancer Res.** 62 (2002) 4879-4883.
18. Ronnstrand, L. Signal transduction via the stem cell factor receptor/c-Kit. **Cell. Mol. Life Sci.** 61 (2004) 2535-2548.

FIGURES

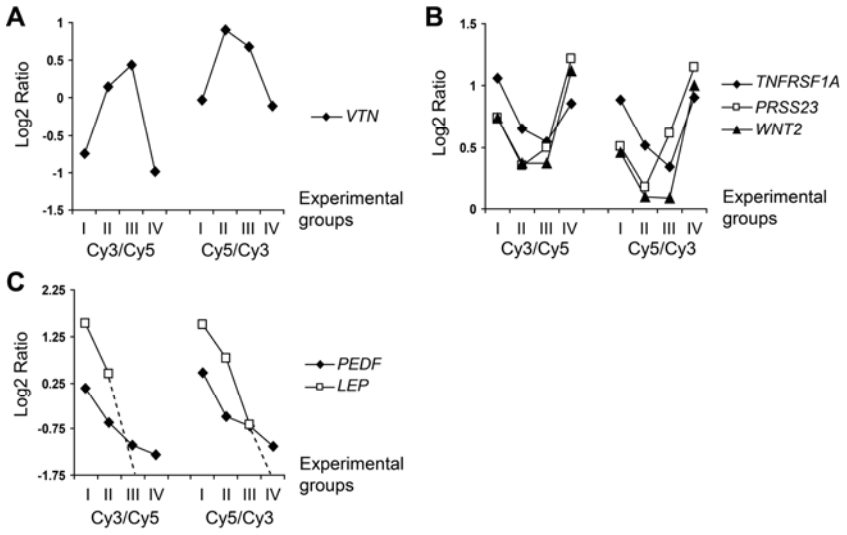

Fig. 1. Secreted factor-encoding genes with a different expression level in hFF after passage 11 (experimental groups, abscissa) plotted as a function of Log2 Ratio (ordinate): bell-shape (A), u-shape (B) and down-regulation (C) patterns. Left panel: Sample Cy3 vs. Reference Cy5. Right panel: Sample Cy5 vs. Reference Cy3. I, passages 6-11; II, passages 12-20; III, passage 25; IV, passage 30. The dashed line in (C) indicates that gene expression of leptin (*LEP*) was below the detection limit. All of the samples shown have their expression altered to the >0.25 range at stage I/II.

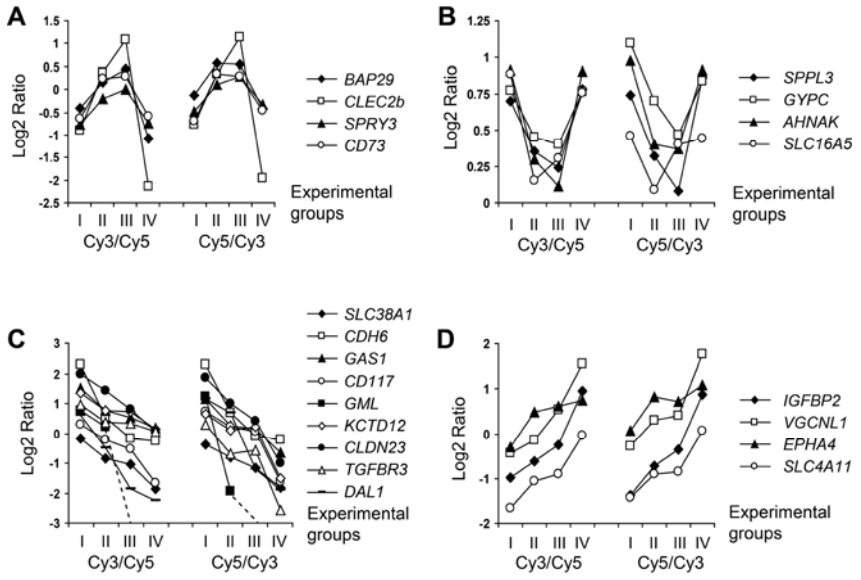

Fig. 2. Cell surface membrane-related genes with a different expression level in hFF after passage 11 (experimental groups, abscissa) plotted as a function of Log2 Ratio (ordinate): bell-shape (A), u-shape (B), down-regulation (C) and up-regulation (D) patterns. Left panel: Sample Cy3 vs. Reference Cy5. Right panel: Sample Cy5 vs. Reference Cy3. I, passages 6-11; II, passages 12-20; III, passage 25; IV, passage 30. The dashed line in (C) indicates that the gene expression of *GML* was below the detection limit. All of the samples shown have their expression altered to the >0.5 range at stage I/II for (A, C) and >0.25 for (B, D).

Tab. 1. Secreted factor-encoding genes with a different expression level in hFF after passage 11.

N	Gene Index	Sample Cy3 *vs.* Reference Cy5				Sample Cy5 *vs.* Reference Cy3			
		I	II	III	IV	I	II	III	IV
1.	***VTN***	-0.743	0.151	0.433	-0.979	-0.028	0.900	0.675	-0.103
2.	*PRSS23*	0.737	0.349	0.496	1.214	0.506	0.172	0.613	1.145
3.	*WNT2*	0.745	0.368	0.373	1.119	0.460	0.093	0.090	1.006
4.	*TNFRSF1A*	1.063	0.657	0.543	0.861	0.886	0.513	0.340	0.907
5.	***PEDF***	0.125	-0.606	-1.095	-1.324	0.476	-0.486	-0.687	-1.132
6.	***LEP***	1.515	0.441	ND	ND	1.492	0.786	-0.667	ND
*	***HOXD4***	-1.389	-0.328	0.156	-0.978	-1.472	-0.301	0.075	-0.981

I, human feeder cells from passages 6-11; II, from passages 12-20; III, from passage 25; IV, from passage 30.
Values, mean Log 2 Ratio.
Only samples with an expression that was different in the >0.25 Log2 Ratio range at stage I/II and a consistent pattern of expression are shown. **Bold** highlights entries with a >0.25 Log2 Ratio range at stage I/II in both Sample Cy3 vs. Reference Cy5 and Sample Cy5 vs. Reference Cy3 datasets. The entries are sorted based on the average value of the Log2 Ratio change of both datasets at stage I/II.
ND, not detected.
* Hoxd4 is not a secreted factor but is believed to affect the secretion process.

SUPPLEMENTAL MATERIALS AND METHODS

Human neonatal foreskin fibroblast cell (hFF) cultures

Human neonatal foreskin fibroblast cells (hFF) were obtained from a commercial source (ATCC; cell line CCD-1112Sk). They were thawed and expanded in hFF medium (Iscove's modified Dulbecco's medium (IMDM, Invitrogen, USA) supplemented with 10% heat-inactivated FCS (Invitrogen) and 0.5% Penicillin/Streptomycin (Invitrogen)). The hFF were grown in 75-cm^2 culture t-flasks which were maintained at 37ºC, in a 5.0% CO_2, 95% humidity atmosphere. Cells were grown to subconfluency (confluency level 85-90%) and passaged by rinsing twice in PBS buffer and incubating for 3 min in pre-warmed 0.05% Trypsin/EDTA solution (Invitrogen). Following Trypsin inhibition with three volumes of hFF medium, the cells were collected by centrifugation.

Human embryonic stem cell (hESC) cultures

Human embryonic stem cells (hESC) were co-cultured with hFF to assess the ability of the latter to support hESC proliferation *in vitro* in an undifferentiated state. Undifferentiated hESC (SA002, Sahlgrenska 2; Cellartis AB, Göteborg, Sweden; see NIH Human Embryonic Stem Cell Registry at http://stemcells.nih.gov/research/registry/cellartis.asp) were maintained on mitotically inactivated hFF. One day prior to hESC passaging, the hFF were inactivated by gamma-irradiation (40 Gy) and plated in the central ring of gelatinized *in vitro* fertilization (IVF) dishes (BD Falcon) at 45,000 cells/cm^2, in hESC proliferation medium (VitroHES media (Vitrolife AB, Sweden) supplemented with 4 ng/ml human recombinant FGF2 (hrbFGF, Biosource International, USA)). The outer rings of the IVF dishes were filled with Dulbecco's modified Eagle medium (DMEM) supplemented with 0.5% Penicillin/Streptomycin (Invitrogen). The hESC were mechanically passaged every 6-8 days by cutting and transferring the colony fragments onto fresh hFF using stem cell knives/transfer pipettes (SweMed Lab International AB, Sweden). Only the hESC colonies presenting an unaltered morphology (indicating a lack of spontaneous differentiation) were passaged (around 10-14 colony fragments per dish, measuring around 0.015 x 0.015 mm). All of the manipulations of the hESC (including the mechanical passaging) were performed over a heating plate (Tokai Hit, Japan) placed over an inverted light microscope (CKX41, Olympus, Japan). One half of the hESC proliferation medium was replaced every other day, and the cells were maintained at 37ºC in a 5.0% CO_2 and 95% humidity atmosphere.

RNA purification and fluorescent dye incorporation

RNA was harvested during passages 6, 7, 8, 9, 10, 11, 12, 13, 14, 15, 20, 25, 30, 34 and 35 of hFF grown under regular conditions. Cells were harvested for RNA isolation at subconfluency for all of the passages, except for passage 35, where the cells were sparser due to the observed cell senescence. For RNA purification, hFF grown in 75-cm^2 culture flasks were rinsed twice in PBS buffer, lysed with 1 ml TRIzol reagent (Invitrogen), scraped, collected and stored at 4ºC until the RNA sample was purified following the RNeasy Kit (QIAGEN, USA) protocol (without carrier RNA); with DNase I (QIAGEN) treatment incorporated to the latter. RNA integrity was tested using both an ND-1000 specrophotometer (NanoDrop, USA) and RNA Nano LabChip/2100 Bioanalyzer system (Agilent Technologies, USA). Total RNA for Sample I and Sample II was prepared by pooling equal quantities of individual total RNA samples purified from hFF harvested after passages 6-11 and 12-15, respectively.

The fluorescent label (24 nmol of the Cyanine 3-CTP (Cy3); PerkinElmer, USA) was incorporated into 500 ng of total RNA by amplification using a Low RNA Input Fluorescent Linear Amplification Kit (Agilent Technologies, USA) according to the manufacturer's protocol. Similarly, 24 nmol of the Cyanine 5-CTP (Cy5; PerkinElmer) fluorescent label was incorporated into a 400-ng sample of Human Universal Reference RNA (Stratagene, USA). In addition, a dye-

swap replicate amplification was performed. The amplified fluorescent cRNA samples were purified using RNeasy mini-columns, and the fluorescence of the eluted products was measured using an ND-1000 spectrophotometer.

Microarray technology

Long oligonucleotide probes (69-71 nucleotides) matching the gene targets of interest were selected from Operon V2 and V3 human AROS sets (Operon Biotechnologies Inc., USA). The NeuroStem 2.0 Chip platform accounts for 1312 oligonucleotides matching genes related to the growth and differentiation of stem cells. Additionally, those markers were supplemented with a large number of different controls, bringing the total unique gene products spotted on a single slide to 11532. All of the unique genes are spotted in quadruplicate on the same slide. Arrays were produced by the SweGene DNA Microarray Resource Centre, Department of Oncology at Lund University (Sweden) using a MicroGrid II 600R arrayer fitted with MicroSpot 10 K pins (Harvard BioRobotics, USA). Printing was performed at 18-20ºC within a humidity (44-49% RH) controlled area on Corning UltraGAPS aminosilane slides (Corning Inc., USA), with 140 μm spot-to-spot center distance and 90-110 μm average spot size. Following printing, the arrays were dried for 48 h and stored in a dessicator until used (shelf life limited to 4 months maximum). Fluorescent dyes (Cy3 or Cy5)-labeled cRNA probes were hybridized using the Pronto! Universal Microarray Hybridization Kit (Corning). After normalization for dye incorporation, the samples were hybridized (against a human universal reference RNA (Stratagene) to UV-cross-linked (800 mJ/cm^2) microarray slides at 42ºC for 17 h using a MAUI hybridization station (BioMicro Systems Inc.), generally following the Pronto! Universal Microarray Hybridization Kit manufacturer's instructions, with several adaptations [1].

Data acquisition and statistical analysis

Immediately following the washing steps, the fluorescence intensities were measured using a confocal laser scanner (G2505B, Agilent Technologies). After image formatting using the Tiff Image Channel Splitter Utility (Agilent Technologies) and grid annotation, a complete set of spots was visually inspected for each slide. Using the GenePix Pro (Molecular Devices Corp., USA) flag function, artifact spots were annotated for each slide. Median pixel intensity minus the median local background for both dyes was used to obtain a test over the reference intensity ratio. Data normalization was performed per array subgrid using a LOWESS curve fitting with a smoothing factor of 0.33 [2, 3]. All of the normalizations, filtering, merging of technical replicates and analyses were performed in the BioArray Software Environment database [4]. To visualize the sample-dependent variation of spot intensities, data was uploaded to the TIGR MultiExperiment Viewer (MEV).

RT-PCR

The primers for RT-PCR were selected from published works or designed using Oligo 4.0 software (Molecular Biology Insight, USA) or Clone Manager Suite 7.1 (Sci Ed Software, USA) and ordered from TAG Copenhagen A/S (Denmark), as the following:

- *GAPDH*, glyceraldehydes-3-phosphate dehydrogenase: 5'-GGA AGG TGA AGG TCG GAG TCA A-3', 5'-GAT CTC GCT CCT GGA AGA TGG T-3';
- *C-KIT*, 5'-AAC GAC ACG CTG GTC CGC TG-3'; 5'-GTA CAC AGA ACT AGA CAC ATC-3' [5];
- *ACTB*, β-actin: 5'-CAT CGA GCA CGG CAT CGT CA-3', 5'-TAG CAC AGC CTG GAT AGC AAC-3';
- *TUBB*, β-tubulin: 5'-CTC ACA AGT ACG TGC CTC GAG-3', 5'-GCA CGA CGC TGA AGG TGT TCA-3';
- *LEP*, leptin: 5´-CCA AGA TGG ACC AGA CAC TG-3´, 5'-GCC ACC ACC TCT GTG GAG TA-3' [6];

- *OCT4*, POU class 5 homeobox 1: 5'-TGG AGT TTG TGC CAG GGT TT-3', 5'-CTT CAC CTT CCC TCC AAC CA-3',
- *RPLP0*, ribosomal phosphoprotein, large, p0: 5'-TTC ATT GTG GGA GCA GAC-3', 5'-CAG CAG TTT CTC CAG AGC-3'.

cDNA was synthesized from 1 µg of total RNA using SuperScript II (Invitrogen), and RT-PCR amplifications were performed using the MiniOpticon system (Bio-Rad, USA) with REDTaq Polymerase (Sigma-Aldrich, USA) essentially as described by the manufacturer. Following initial denaturation for 5 min at 95ºC, DNA amplifications were performed for 25 cycles of 1 min at 95ºC, 1 min at 57ºC, and 1 min at 72ºC. The final extension was 5 min at 72ºC. Twenty µl volumes of RT-PCR products were analyzed by electrophoresis using 1.0% Agarose gels and visualized by Ethidium Bromide staining. qPCR was performed using SYBR Green (Fermentas, Canada). The measured transcript levels were normalized to *RPLP0*. The samples were run in triplicate.

Serial Analysis of Gene Expression (SAGE) cross-library analysis

In silico analysis based on Serial Analysis of Gene Expression (SAGE) technology was employed to compare data generated from the microarray with an alternative method. A basic protocol for SAGE library construction and handling was published elsewhere [7]. The SAGE catalogs (i.e. libraries of sequenced tags) for the analysis were of the primary hFF passage (passage 0; GSM1), of passages 15-18 (GSM14916) and of MEF passage 3 (GSM7759; [8]). They were downloaded from the Gene Expression Omnibus (GEO) database (National Center for Biotechnology Information, NCBI). Non-informative sequences were extracted from the downloaded SAGE libraries when detected [9], and tags per million (tpm) values were re-calculated accordingly, as the transcript's raw tag count was divided by the number of tags in the library and multiplied by one million. We then employed the SAGEmap annotation tool to identify the most reliable SAGE tags for the genes of interest. These were matched to downloaded SAGE libraries using the MS Access software package Query function. Individual queries were merged, and calculations of the relative expressions of individual transcripts were performed using normalized tpm values.

ELISA studies of PEDF secretion in hFF

In order to investigate the levels of secreted PEDF from the hFF, ELISA was performed on early-, mid- and late-stage hFF. The cells used were from passages 9, 16 and 21. As a negative control, fresh culture medium was used. Supernatant was collected from 100000 plated cells following 24 h of culture. ELISA was performed according to the manufacturer's protocol (BioProducts MD, Middletown, MD) in duplicate. Briefly, 100 µl of a 7-fold dilution BSA standard curve ranging from 0 mg/ml to 1.75 mg/ml and 7-fold dilution series of the supernatant from the 3 passages was pipetted into a multi-well microplate. The microplate was incubated at 37ºC for one hour. The supernatant was removed and the wells were rinsed five times with PBS. 100 µl of PEDF detector antibody was added to each well and incubated at 37ºC for one hour. The wells were washed 5 times with PBS and 100 µl Streptavidin Peroxidase solution was added to each well except the substrate blank. Following 30 min incubation at 37ºC, the wells were washed 5 times in PBS. Finally, 100 µl of TMB substrate was added to each well and following 20 min incubation at room temperature, the reaction was stopped using 100 µl of Stop Solution. The optical density was immediately measured at 450 nm using a microplate reader. The concentration was determined by performing regression analysis and plotting the mean optical densities versus the concentration of the PEDF antigen standard. The values were normalized against the control (i.e. hFF culture medium).

SUPPLEMENTAL REFERENCES

1. Anisimov, S.V. Application of DNA microarray technology to gerontological studies. **Methods Mol. Biol.** 371 (2007) 249-265.
2. Cleveland, W.S. and Devlin, S.J. Locally weighted regression: an approach to regression analysis by local fitting. **J. Am. Stat. Assoc.** 83 (1988) 596-610.
3. Yang, Y.H., Dudoit, S., Luu, P., Lin, D.M., Peng, V., Ngai, J. and Speed, T.P. Normalization for cDNA microarray data: a robust composite method addressing single and multiple slide systematic variation. **Nucleic Acids Res.** 30 (2002) e15.
4. Saal, L.H., Troein, C., Vallon-Christersson, J., Gruvberger, S., Borg A. and Peterson, C. BioArray Software Environment (BASE): a platform for comprehensive management and analysis of microarray data. **Genome Biol.** 3 (2002) software0003.1-0003.6.
5. Rassidakis, G.Z., Georgakis, G.V., Oyarzo, M., Younes, A. and Medeiros, L.J. Lack of c-kit (CD117) expression in CD30+ lymphomas and lymphomatoid papulosis. **Mod. Pathol.** 17 (2004) 946-953.
6. Aparicio, T., Kermorgant, S., Darmoul, D., Guilmeau, S., Hormi, K., Mahieu-Caputo D. and Lehy, T. Leptin and Ob-Rb receptor isoform in the human digestive tract during fetal development. **J. Clin. Endocrinol. Metab.** 90 (2005) 6177-6184.
7. Anisimov, S.V., Tarasov, K.V. and Boheler, K.R. Serial Analysis of Gene Expression (SAGE): Detailed protocol and analysis. in: **Cell Biology: A Laboratory Handbook, 3rd Edition** (Celis, J., ed.), Academic Press, San Diego, CA, USA, 2005, IV.14.1-IV.14.10.
8. Wiese, C., Rolletschek, A., Kania, G., Navarrete-Santos, A., Anisimov, S.V., Steinfarz, B., Tarasov, K.V., Brugh, S.A., Zahanich, I., Rüschenschmidt, C., Beck, H., Blyszczuk, P., Czyz, J., Heubach, J.F., Ravens, U., Horstmann, O., St-Onge, L., Braun, T., Brüstle, O., Boheler K.R. and Wobus, A.M. Signals from embryonic fibroblasts induce adult intestinal epithelial cells to form nestin-positive cells with proliferation and multilineage differentiation capacity in vitro. **Stem Cells.** 24 (2006) 2085-2097.
9. Anisimov, S.V. and Sharov, A.A. Incidence of "quasi-ditags" in catalogs generated by Serial Analysis of Gene Expression (SAGE). **BMC Bioinformatics.** 5 (2004) 152.

Suppl. Tab. 1. Cell surface membrane-related genes with a different expression level in hFF after passage 11.

N	Gene symbol	Sample Cy3 *vs.* Reference Cy5				Sample Cy5 *vs.* Reference Cy3			
		I	II	III	IV	I	II	III	IV
1.	***CLEC2B***	-0.895	0.359	1.086	-2.132	-0.766	0.332	1.136	-1.946
2.	***CD73***	-0.630	0.225	0.298	-0.601	-0.693	0.338	0.295	-0.472
3.	*CNTNAP2*	-0.743	-0.260	ND	ND	-1.228	-0.111	ND	ND
4.	***EPHA4***	-0.289	0.473	0.627	0.749	0.064	0.818	0.725	1.077
5.	***BAP29***	-0.419	0.153	0.455	-1.068	-0.120	0.571	0.547	-0.401
6.	*TAF1A*	-1.555	-0.824	-0.819	-1.540	-0.349	0.094	-0.032	-0.525
7.	*CDCP1*	-0.866	-0.160	-0.685	-1.633	-0.355	0.105	-0.427	-1.021
8.	***SPRY3***	-0.766	-0.215	0.011	-0.742	-0.498	0.116	0.294	-0.327
9.	***SLC4A11***	-1.653	-1.062	-0.901	-0.050	-1.416	-0.892	-0.858	0.060
10.	*TMTC3*	0.222	0.858	0.831	-1.516	0.651	1.090	1.010	0.612
11.	*IGFBP2*	-0.988	-0.627	-0.245	0.954	-1.381	-0.716	-0.353	0.868
12.	*DST*	0.260	0.726	0.752	-0.348	0.463	0.955	0.912	-0.168
13.	*ANXA1*	0.985	1.535	1.035	-0.582	1.242	1.578	1.849	-0.410
14.	*ALCAM*	0.502	0.951	1.241	-0.444	0.546	0.977	1.306	-0.449
15.	*B4GALT7*	-0.131	0.349	0.315	-1.576	0.125	0.514	0.345	-1.015
16.	*VGCNL1*	-0.433	-0.141	0.532	1.557	-0.262	0.303	0.418	1.755
17.	*ATP2B1*	0.020	0.390	0.571	-0.580	-0.102	0.376	0.569	-0.713
18.	*PTGER2*	-0.155	0.236	-0.099	-0.661	0.116	0.545	-0.150	-0.520
19.	*RTTN*	-0.987	-0.494	-0.178	-1.220	-0.765	-0.453	-0.355	-1.025
20.	*OSTM1*	-0.915	-0.512	0.107	-1.445	-0.969	-0.616	0.006	-1.439
21.	*FAM18B*	0.631	0.925	1.518	-0.027	0.291	0.695	1.363	0.365
22.	*MELK*	-0.802	-0.402	-0.482	-2.288	0.076	0.360	0.069	-1.929
23.	*STXBP3*	-0.208	0.124	0.742	-1.431	-0.301	0.027	0.572	-1.255
24.	*ARF6*	0.410	0.695	0.865	-0.262	0.598	0.908	0.954	0.211
25.	*MMP1*	0.687	0.972	0.491	-1.284	0.826	1.080	0.474	-1.114
26.	*PLSCR1*	-0.247	-0.583	-0.772	-2.129	-0.239	-0.498	-0.815	-1.929
27.	*SERPINB2*	0.578	0.250	-0.213	-1.157	0.458	0.147	-0.351	-0.785
28.	*RBIG1*	0.878	0.582	0.232	-0.238	0.936	0.563	0.290	0.141
29.	*GYPC*	0.776	0.451	0.401	0.766	1.094	0.704	0.471	0.838
30.	*TOX*	0.408	0.083	0.074	-1.325	0.401	-0.014	0.197	-1.233
31.	*SPPL3*	0.700	0.358	0.241	0.781	0.738	0.322	0.079	0.867
32.	*LGALS3*	0.962	0.576	0.465	-0.212	0.905	0.531	0.298	-0.105
33.	***CD117***	0.304	-0.233	-0.528	-1.654	0.714	0.210	0.066	-1.629
34.	***SLC38A1***	-0.183	-0.859	-1.053	-1.849	-0.382	-0.789	-1.156	-1.837
35.	***SLC16A5***	0.891	0.154	0.303	0.757	0.464	0.090	0.403	0.442
36.	***KCTD12***	1.338	0.766	0.710	0.147	0.666	0.087	0.225	-1.504
37.	***AHNAK***	0.912	0.300	0.113	0.906	0.974	0.403	0.374	0.915
38.	***CLDN23***	1.971	1.434	0.806	0.045	1.868	0.996	0.421	-1.005
39.	***TFGBR3***	0.946	0.369	0.342	0.043	0.310	-0.697	-0.580	-2.560
40.	***DAL1***	0.606	-0.487	-1.862	-2.255	1.170	0.677	-1.183	-1.912
41.	***GAS1***	1.515	0.781	0.518	0.164	1.174	0.243	0.147	-0.661
42.	***CDH6***	2.294	0.540	-0.169	-0.262	2.297	0.681	-0.093	-0.201
43.	***GML***	0.767	0.206	ND	ND	1.247	-1.931	ND	ND

I, human feeder cells from passages 6-11; II from passages 12-20; III from passage 25; IV from passage 30.
Values, mean Log 2 Ratio.
Only samples with an expression that was different in the >0.25 Log2 Ratio range at stage I/II and a consistent pattern of expression are shown. **Bold** highlights entries with a >0.25 Log2 Ratio range at stage I/II in both Sample Cy3 vs. Reference Cy5 and Sample Cy5 vs. Reference Cy3 datasets. The entries are sorted based on the average value of the Log2 Ratio change of both datasets at stage I/II.
ND, not detected.

Suppl. Tab. 2. Unique genes encoding secreted, secretion-related and cell surface membrane-related products identified in one of the three available SAGE libraries constructed from feeder cells.

N	Tags	Sp.	Gene symbol	Category	TQ	GSM14916 hFC, p.0		GSM1 hFC, p.15-18		GSM7759 MEF, p.3	
						Count	tpm	Count	tpm	Count	tpm
1.	AATGTACAAG	Mm	*AHNAK*	CSM	*					24	370
2.	ATTAAGAAAA	Hs				2	35				
3.	TACCGCGTCA	Mm	*ALCAM*	CSM						1	15
4.	CTGAAAAATA	Hs	*ANXA1*	CSM		1	17				
5.	GGCTTAAGTA	Mm			*					17	262
6.	CAGACTATGT	Hs	*ARF6*	CSM		2	35	1	103		
7.		Mm			*					11	170
8.	GTTAACCTCT	Hs				1	17				
9.	CCGAAAGGGA	Mm	*ATP2B1*	CSM	*					2	31
10.	CTTAGTGTGT	Hs			*	2	35				
11.	GTCCTGAACA	Hs				3	52				
12.	CCGGAATGTG	Hs	*B4GALT7*	CSM	*	1	17	1	103		
13.	GTAAAGATGA	Hs	*BAP29*	CSM				1	103		
14.	TAGAAGTAGT	Mm			*					1	15
15.	AGCCTGCTCA	Hs	*CD73*	CSM	*	4	70	2	205		
16.	ATTACTCAGG	Hs				2	35				
17.	TGTTTGTTTT	Hs				1	17				
18.	TTGGTTTCCT	Mm			*					1	15
19.	CCCTTGGCGT	Hs	*CDCP1*	CSM		1	17				
20.	GCCTTGGTAA	Hs				1	17				
21.	ACCATCCTGC	Hs	*CDH6*	CSM	*	1	17				
22.	AGAACTTACC	Mm								3	46
23.	TTTGGAAGAC	Hs				1	17				
24.	AATGAATGAA	Hs	*CNTNAP2*	CSM		1	17	1	103		
25.	TGTGATGTTA	Mm								1	15
26.	CCTTTCATAG	Mm	*DAL1*	CSM	*					5	77
27.	GTGAATGTAT	Hs			*	1	17				
28.	GCGTTCACAC	Mm	*DST*	CSM						14	216
29.	AACTTTAGGT	Hs	*EPHA4*	CSM	*	1	17				
30.	TCATAATGAG	Hs	*FAM18B*	CSM	*	5	87				
31.	AGGAATCCAC	Mm	*GAS1*	CSM	*					15	231
32.	TACATCAGTA	Hs			*	2	35				
33.	TATGAAAGTC	Hs				1	17				
34.	TTCGGCCCTC	Mm								13	200
35.	GGGCCCCCTG	Hs	*GYPC*	CSM	*	1	17	3	308		
36.	TGTTTGACCT	Mm								1	15
37.	GCCTGTACAA	Hs	*IGFBP2*	CSM	*	2	35	2	205		
38.	TATTTATATT	Mm			*					1	15
39.	GTGAAACCCC	Hs	*LEP*	Secr.	*	163	2838	63	6467		
40.	ATATAATCTG	Hs	*LGALS3*	CSM		5	87	2	205		

N	Tags	Sp.	Gene symbol	Category	TQ	GSM14916 hFC, p.0		GSM1 hFC, p.15-18		GSM7759 MEF, p.3	
						Count	tpm	Count	tpm	Count	tpm
41.	TTCACTGTGA	Hs			*	16	279	6	616		
42.	GGCTTGGTAT	Mm	*MELK*	CSM						1	15
43.	TGGTTTTGTA	Hs			*	5	87				
44.	TGCAGTCACT	Hs	*MMP1*	CSM	*	20	348	3	308		
45.	TGCAAAGTGA	Mm	*OSTM1*	CSM	*					1	15
46.	TTCAATTCTG	Hs				2	35				
47.	AAATGTTTAG	Hs	*PLSCR1*	CSM	*	1	17				
48.	CCTGTCTGCA	Hs	*PRSS23*	Secr.	*	2	35	1	103		
49.	CGTCTTCTTG	Mm								5	77
50.	TTCTTATTTT	Hs				5	87	2	205		
51.	TAAATGTAAA	Hs	*PTGER2*	CSM	*	1	17				
52.	GGGGCTTCCC	Hs	*RBIG1*	CSM		1	17				
53.	AGAGAGAGAA	Hs	*RTTN*	CSM	*	2	35				
54.	AAGCTACAGT	Mm	*SERPINF1 /PEDF*	Secr.						58	894
55.	ATGTCAGATC	Mm								1	15
56.	TAGCACACCA	Mm	*SLC38A1*	CSM						3	46
57.	AGCTGGGCGT	Mm	*SLC4A11*	CSM						1	15
58.	GCTGACTCAG	Hs			*	5	87	3	308		
59.	CACTGGTTCA	Mm	*SPPL3*	CSM						1	15
60.	CCCTCACTCC	Hs				1	17				
61.	CCTGCTCACG	Mm								4	62
62.	GAGCAGCGTG	Mm			*					8	123
63.	AACATTCTAA	Hs	*STXBP3*	CSM	*	1	17				
64.	AAACTGACAG	Hs	*TFGBR3*	CSM		1	17				
65.	GTCTTTGTGA	Mm			*					1	15
66.	TAGAGAGTTT	Hs	*TMTC3*	CSM		3	52				
67.	TATGTACACA	Mm			*					2	31
68.	TTTCTGCCTT	Hs				2	35				
69.	CAGGGTTCTT	Mm	*TNFRSF1A*	Secr.						1	15
70.	CTGGAAGCCT	Mm			*					25	385
71.	TTACACTAAT	Hs			*	3	52				

Sp., Species: Hs, *Homo sapiens*; Mm, *Mus musculus*.
Category: CSM, cell surface membrane; Secr., secretion.
TQ, Tag quality: asterisk (*) denotes tags with only 1 reliable gene mapping.
tpm, normalized tag per million value.
CAGACTATGT is the sole tag with an identical sequence for both *Homo sapiens* and *Mus musculus*. Note the degree of redundancy in the entries, with few SAGE tags linking to the same gene in each species.

SUPPLEMENTARY FIGURES

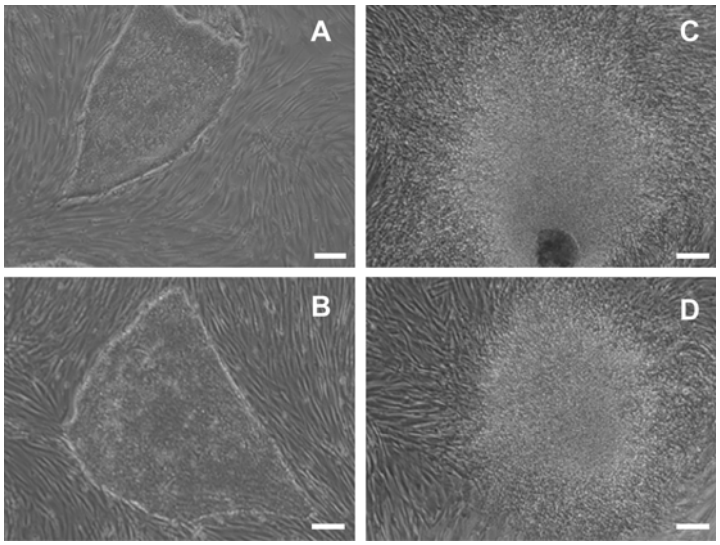

Suppl. Fig. 1. Human embryonic stem cells (hESC) cultured on hFF with low (≤11, A, B) and very high (≥25, C, D) passage numbers. Massive spontaneous differentiation of the hESC is evident in C and D, converging to 100%. Scale bars = 100 μm.

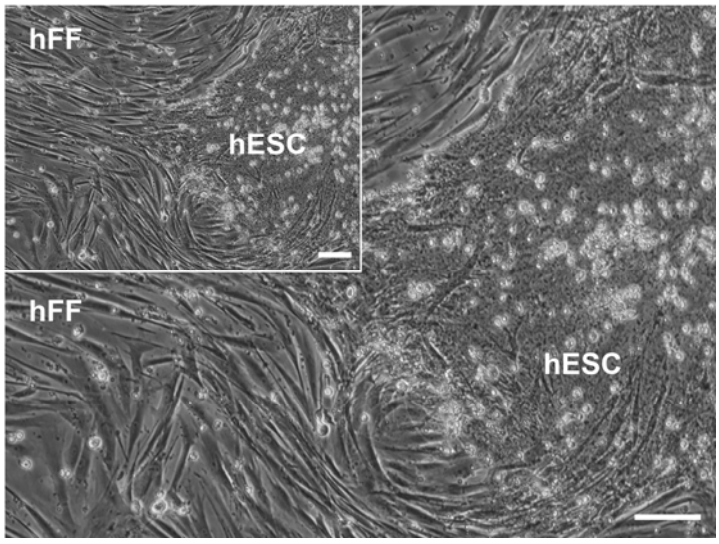

Suppl. Fig. 2. Human embryonic stem cells (hESC) cultured on hFF with a very high (30) passage number. Massive cell death of hESC is evident (note numerous bright rounded cells) in the formed colony, which has an altered morphology (shown in lower magnification in the insert). Scale bars = 100 μm.

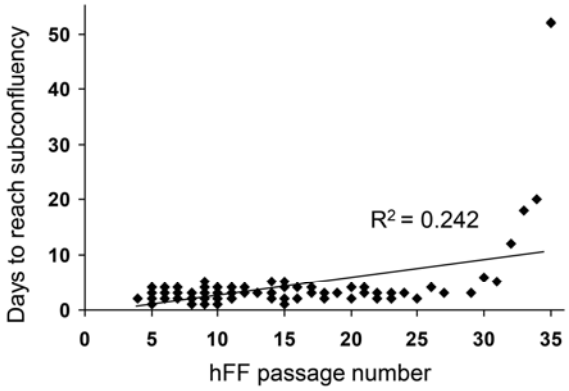

Suppl. Fig. 3. The growth rate of hFF as estimated by the time required for the hFF to reach subconfluency once seeded. The trendline is shown for the whole dataset, with R2 = 0.261 for passage number ≥ 10 and R2 = 0.582 for passage number ≥ 25, suggesting that the hFF growth rate decreases past passage number 25. The subconfluency stage could not be reached for the sole entry with passage number = 35, thus emphasizing the underestimation of the R2 values observed.

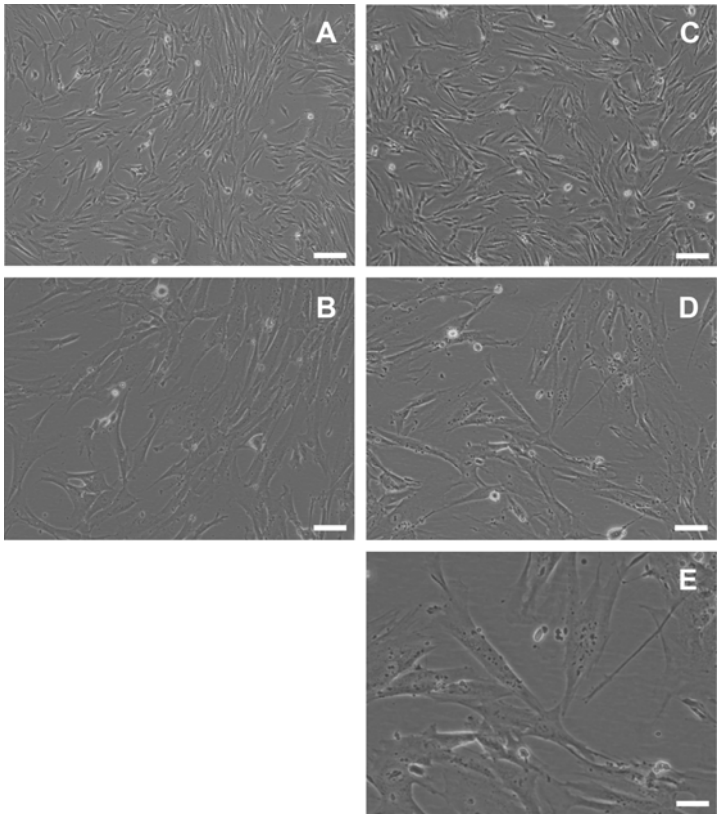

Suppl. Fig. 4. The morphology of hFF with low (≤11, A, B) and very high (≥25, C-E) passage numbers. Scale bars = 100 μm (A, C), 40 μm (B, D) and 20 μm (E).

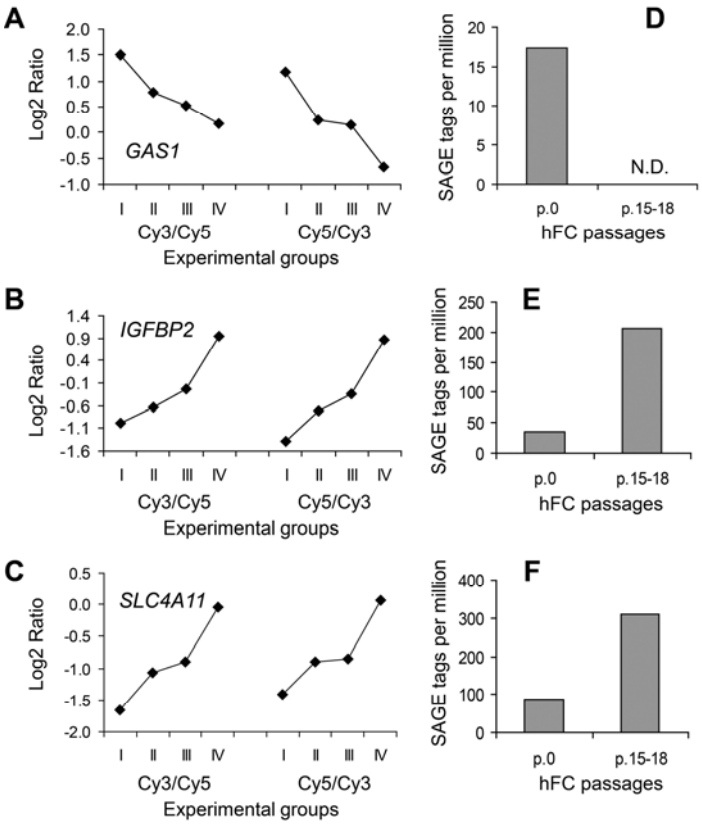

Suppl. Fig. 5. Gene targets with different expression levels in human feeder cells after passage 11 as detected by microarray analysis (A-C) and SAGE technology (D-F). (A-C) Gene expression in experimental groups (abscissa) is plotted as a function of Log2 Ratio (ordinate); Left panel: Sample Cy3 vs. Reference Cy5; Right panel: Sample Cy5 vs. Reference Cy3. I, passages 6-11; II, passages 12-20; III, passage 25; IV, passage 30. (D-F) Normalized expression in SAGE libraries is plotted as a function of the tag per million (tpm) value (ordinate) for the primary hFC culture (p.0) and that cultured for 15-18 passages. *GAS1*, Growth arrest-specific 1 (A, D); *IGFBP2*, Insulin-like growth factor binding protein 2, 36 kDa (B, E); *SLC4A11*, Solute carrier family 4 sodium bicarbonate transporter-like member 11 (C, F). N.D., not detected.

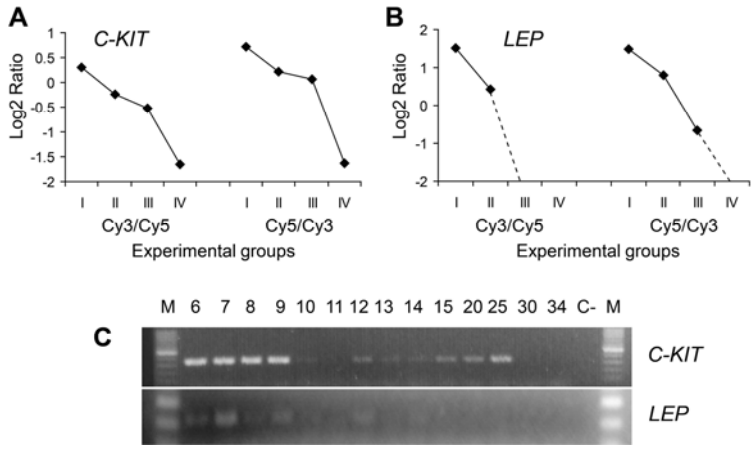

Suppl. Fig. 6. The expressions of *C-KIT* and *LEP* in hFF as measured using the microarray (A, B) and RT-PCR (C) techniques. (A, B) Gene expression in experimental groups (abscissa) is plotted as a function of the Log2 Ratio (ordinate); Left panel: Sample Cy3 vs. Reference Cy5; Right panel: Sample Cy5 vs. Reference Cy3. I, passages 6-11; II, passages 12-20; III, passage 25; IV, passage 30. The dotted line in B indicates that the gene expression of *LEP* was below the detection limit. Both genes had different expression levels in the >0.5 range at stage I/II. (C) M, DNA ladder; hFF at passage 6-15, 20, 25, 30 and 34; C-, no template negative control.